HHS Public Access

Author manuscript

Glia. Author manuscript; available in PMC 2023 October 01.

Published in final edited form as:

Glia. 2022 October ; 70(10): 1886–1901. doi:10.1002/glia.24226.

Deletion of RE1-silencing transcription factor in striatal astrocytes exacerbates manganese-induced neurotoxicity in mice

Edward Pajarillo[1], **Mark Demayo**[1], **Alexis Digman**[1], **Ivan Nyarko-Danquah**[1], **Deok-Soo Son**[2], **Michael Aschner**[3,4], **Eunsook Lee**[1,*]

[1]Department of Pharmaceutical Sciences, Florida A&M University, Tallahassee, FL, USA

[2]Department of Biochemistry and Cancer Biology, Neuroscience and Pharmacology, Meharry Medical College, Nashville, Tennessee, USA

[3]Department of Molecular Pharmacology, Albert Einstein College of Medicine, Bronx, New York, New York, USA,

[4]Laboratory for Molecular Nutrition of the Institute for Personalized Medicine, Sechenov First Moscow State Medical University, Moscow, Russia

Abstract

Chronic manganese (Mn) overexposure causes a neurological disorder, referred to as manganism, exhibiting symptoms similar to parkinsonism. Dysfunction of the repressor element-1 silencing transcription factor (REST) is associated with various neurodegenerative diseases such as Parkinson's disease, Alzheimer's disease, and Mn-induced neurotoxicity, but its cellular and molecular mechanisms have yet to be fully characterized. Although neuronal REST is known to be neuroprotective, the role of astrocytic REST in neuroprotection remains to be established. We investigated if astrocytic REST in the striatal region of the mouse brain where Mn preferentially accumulates plays a role in Mn-induced neurotoxicity. Striatal astrocytic REST was deleted by infusion of adeno-associated viral vectors containing sequences of the glial fibrillary acidic protein promoter-driven Cre recombinase into the striatum of $REST^{flox/flox}$ mice for 3 weeks, followed by Mn exposure (30 mg/kg, daily, intranasally) for another 3 weeks. Striatal astrocytic REST deletion exacerbated Mn-induced impairment of locomotor activity and cognitive function with further decrease in Mn-reduced protein levels of tyrosine hydroxylase and glutamate transporter 1 (GLT-1) in the striatum. Astrocytic REST deletion also exacerbated the Mn-induced proinflammatory mediator COX-2, as well as cytokines such as TNF-α, IL-1β, and IL-6, in the striatum. Mn-induced detrimental astrocytic products such as proinflammatory cytokines on neuronal toxicity were attenuated by astrocytic REST overexpression, but exacerbated by REST

*To whom correspondence should be addressed: Eunsook Lee, R.Ph, Ph.D., Department of Pharmaceutical Sciences, Florida A&M University, Tallahassee, FL, USA 32301. eunsook.lee@famu.edu.

Author contributions: Conceptualization – EP, EL, Data Curation – EP, MD, AD, IND, Formal analysis – EP, Funding acquisition – EL, MA, DSS, Investigation – EP, Methodology – EP, Project administration – EL, Resources – EL, Software – EP, Supervision – EL, Validation – EP, EL, DSS, MA, Visualization – EP, Writing – original draft – EP, EL, Writing – review & editing – EP, MD, AD, IND, DSS, MA, EL.

Conflict of interest statement

The authors declare no conflicts of interest with the contents of this article.

inhibition in an *in vitro* model using primary human astrocytes and Lund human mesencephalic (LUHMES) neuronal culture. These findings indicate that astrocytic REST plays a critical role against Mn-induced neurotoxicity by modulating astrocytic proinflammatory factors and GLT-1.

Graphical Abstract

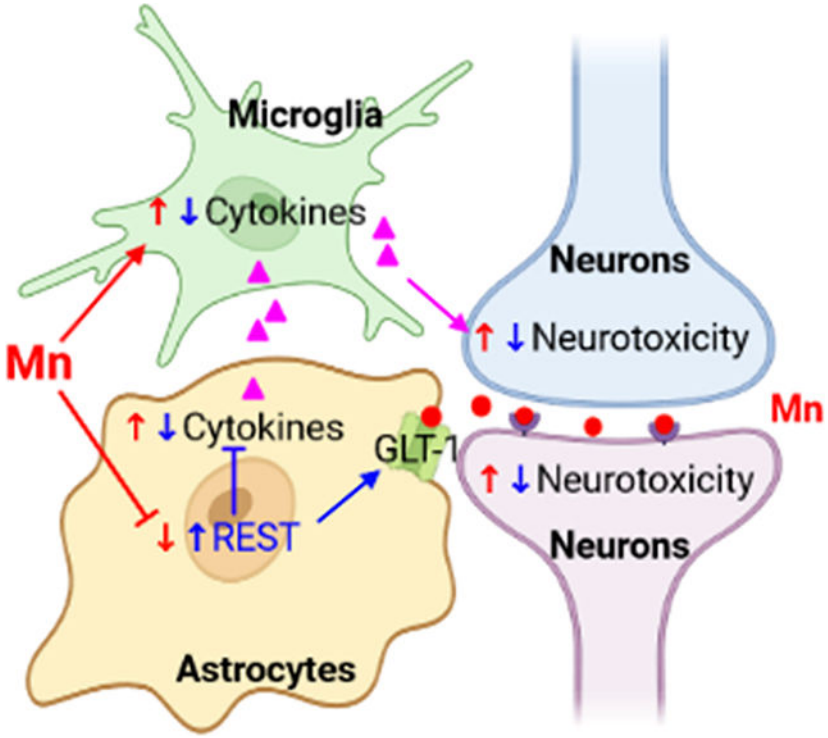

Keywords

adeno-associated viral (AAV) vector; astrocytes; cytokines; GLT-1; neuroinflammation; manganese; neurotoxicity; NRSF; REST

1. Introduction

Chronic exposure to elevated levels of manganese (Mn) in environmental settings such as contaminated air and water, as well as occupational settings, such as alloy productions in manufactures, may lead to a neurological disorder referred to as manganism, characterized by symptoms analogous to those seen in Parkinson's disease (PD), such as tremor, dystonia, and gait (Palm, Metsis, & Timmusk, 1999).

Experimental studies have also shown that Mn-induced neurotoxicity, such as motor deficits in various animal models, including non-human primates, rats, and mice (Guilarte et al., 2006; Inoue, Tsukada, & Barbeau, 1975; Pajarillo et al., 2018). Mn has also been shown to induce impairment in non-motor neuronal functions, including olfaction in humans (Banta & Markesbery, 1977; Bouabid, Fifel, Benazzouz, & Lakhdar-Ghazal, 2016; Zoni, Bonetti, & Lucchini, 2012). Moreover, growing evidence has shown that Mn exposure contributes

to the development of Alzheimer's disease (AD) and dementia by causing impairment in memory and cognitive function, as well as speech changes (Banta & Markesbery, 1977; Tong et al., 2014). These are supported by studies corroborating elevated Mn levels in the plasma and cerebrospinal fluid of AD patients (Basun, Forssell, Wetterberg, & Winblad, 1991), as well as children with lower memory capability (Carvalho et al., 2018) and IQ (McGann et al., 2021). Thus, investigating the molecular mechanisms underlying Mn-induced neurotoxicity is critical for developing neuro-therapeutics to prevent or treat the aforementioned neurological disorders.

Mn enters the brain via various transporters including divalent metal transporter-1 (DMT-1), and accumulates preferentially in basal ganglia such as globus pallidus, striatum, and substantia nigra (Newland, Ceckler, Kordower, & Weiss, 1989) although it does in other regions as well (Pajarillo, Johnson, et al., 2020). Mn is predominantly taken up by astrocytes among neural cell types in the brain (Aschner, Vrana, & Zheng, 1999), implying that astrocytes may play a critical role in Mn-induced neurotoxicity (Aschner, Gannon, & Kimelberg, 1992). The molecular mechanisms of Mn-induced toxicity in astrocytes have been reported, and they include mitochondrial dysfunction, oxidative stress, inflammation, and excitotoxicity (for review, see (Pajarillo, Nyarko-Danquah, et al., 2021)), similar to human neurological disorders, including PD and AD (for review, see (Emerit, Edeas, & Bricaire, 2004)). Given these findings, it is vital to identify factors that play a critical role in the dysregulation of these molecular functions in multiple neurological disorders including Mn-induced neurotoxicity.

The repressor element-1 silencing transcription factor (REST), also known as neuron restrictive silencing factor (NRSF), is a member of the zinc finger-type transcription factors (Palm, Belluardo, Metsis, & Timmusk, 1998). REST modulates a variety of genes associated with ion channels, neurotransmitter receptors, synaptic vesicle proteins, and adhesion molecules (for review, see (Schoenherr, Paquette, & Anderson, 1996)). REST was initially reported as a repressor of multiple neuron-specific genes in neuronal precursor cells during development, and in non-neuronal cells and tissues (Chen, Paquette, & Anderson, 1998; Chong et al., 1995; Schoenherr & Anderson, 1995). REST binds to a 21-bp *cis*-regulatory element known as repressor element-1/neuron restrictive silencing element (RE1/NRSE) to regulate more than 2,000 target genes (Bruce et al., 2009). Although REST was initially known to repress target genes, growing evidence shows that REST also activates target genes in neurons and astrocytes (Abramovitz et al., 2008; Bessis, Champtiaux, Chatelin, & Changeux, 1997; Pajarillo, Digman, et al., 2021; Pajarillo, Rizor, Son, Aschner, & Lee, 2020). We have recently reported that REST activated tyrosine hydroxylase (TH) in neuronal cells by direct binding to its *cis*-element of the TH promoter with parallel increases of TH promoter activities, mRNA and protein levels (Pajarillo, Rizor, et al., 2020). REST also directly activated excitatory amino acid transporter 2 (EAAT2) in astrocytes by increasing EAAT2 expression at the transcriptional level (Pajarillo, Digman, et al., 2021).

Recent studies have reported that REST contributed to neuroprotection in several neurodegenerative diseases, including PD (Huang et al., 2019; Kawamura et al., 2019; Yu et al., 2013), and AD (T. Lu et al., 2014) in human brains and mouse models, as well as Mn-induced neurotoxicity in a neuronal culture model (Pajarillo, Rizor, et al., 2020).

Dysregulation of REST has been shown in postmortem human brain by its sequestration with Lewy bodies (LB), a pathological hallmark of PD and dementia (Kawamura et al., 2019). High levels of REST expression have been associated with protection against stress and AD by reducing proapoptotic proteins and enhancing antiapoptotic and antioxidative factors in both human and mouse brains (T. Lu et al., 2014). Although the protective effects of neuronal REST in neurodegenerative disorders has been reported, the role of astrocytic REST in contributing to neuroprotection is not much known.

While the *in vitro* study of the role of astrocytic REST provides more insight into the molecular mechanistic understanding, the *in vivo* model of astrocytic REST in the brain may provide integrative function of astrocytic REST. It has been reported that astrocyte-specific deletion of REST exacerbated a PD toxin 1-methyl-4-phenyl-1,2,3,6-tetrahydropyridine hydrochloride (MPTP)-induced dopaminergic neuronal loss in substantia nigra of the mouse brain compared to those in the wild type (WT) mice (Li et al., 2020). Astrocytic REST deletion also increased MPTP-induced proinflammatory cytokines, as well as activation of astrocyte and microglia, indicating a protective role of astrocytic REST in MPTP-induced inflammation. REST has shown to directly regulate a set of genes associated with innate immunity and inflammation in human hippocampus (McGann et al., 2021), while its dysregulation of inflammation was implicated in aging-related neuropathology such as AD, further suggesting a critical role of REST in balancing inflammation in the brain. Moreover, we found that REST activated the astrocytic glutamate transporter 1 (GLT-1, EAAT2 in humans) by directly binding to the EAAT2 promoter region and following transcriptional expression, resulting in functional increase of glutamate uptake in astrocytes (Pajarillo, Digman, et al., 2021). This astrocytic REST-induced elevation of EAAT2 protein levels attenuated the glutamate-induced neurotoxicity in LUHMES dopaminergic neuronal cells.

The critical role of astrocytes in the brain function is well established, including the regulation of glutamate homeostasis via astrocytic glutamate transporters (Rothstein et al., 1996). Yet, the role of astrocytic REST, particulary associated with Mn-induced neurotoxicity, in the striatal region-specific has not been studied. Investigating astrocytic REST functions in the brain region-specific manner might be complexed by a variety of neural cell types, activities and functions in the brain microenvironment (for review, see (Poulin, Tasic, Hjerling-Leffler, Trimarchi, & Awatramani, 2016)). We have developed an animal model of astrocyte-specific and striatal-specific REST deletion in the mouse brain by applying AAV-GFAP-Cre-GFP vectors into the dorsal striatum of REST-floxed mice (Pajarillo, Johnson, et al., 2020).

In this study, we investigated the effects of astrocyte-specific deletion of REST in the striatum of Mn-exposed mice to test if astrocytic REST modulates Mn toxicity. The rationales of choosing the striatal region for astrocytic REST deletion are that (1) Mn is preferentially accumulated in globus pallidus and striatum where dopaminergic nerve terminals are innervated, (2) Mn exposure in the striatum induces striatal excitotoxic lesions (Brouillet, Shinobu, McGarvey, Hochberg, & Beal, 1993), as well as dopaminergic neuronal death in substantia nigra of rats (Zhao et al., 2009), and (3) PD toxins such as MPTP are known to target dopaminergic nerve terminals in the striatum to cause dopaminergic neurodegeneration retrogradely (Przedborski & Vila, 2001). Our findings demonstrate, for

the first time, that astrocytic REST deletion in the striatum of the mouse brain exacerbated Mn-induced toxicity, including nigrostriatal dopaminergic dysfunctions, motor deficits and cognitive impairment along with molecular changes in inflammation and glutamate transporter GLT-1.

2. Materials and methods

2.1. Chemicals, antibodies, and plasmid vectors

Manganese chloride ($MnCl_2$), dimethyl sulfoxide (DMSO), and resazurin sodium salt (R7017) were purchased from MilliporeSigma (St. Louis, MO). All cell culture media, including trypsin-EDTA, Minimum Essential Media (MEM), Dulbecco's Modified Eagle Medium (DMEM), DMEM/F-12, and Opti-MEM, were obtained from Gibco (Carlsbad, CA). The chloromethyl derivative of 2',7'-dichlorodihydrofluorescein diacetate (CM-H2DCFDA), a ROS molecular probe was purchased from Invitrogen (Carlsbad, CA). Antibodies for REST (07–579) and NeuN (ABN78) were acquired from MilliporeSigma. Antibodies for EAAT2 (sc-365634), REST (sc-374611), TH (sc-25269), GAD65/67 (sc-365180), COX-2/PTGS2 (ab15191), TNF-α (sc-52746), and β-actin (sc-47778) were obtained from Santa Cruz Biotechnology (Santa Cruz, CA). Antibodies for GFP (ab13970), Cre recombinase (ab216262), EAAT2/GLT-1 (ab41621), GFAP (ab4674), Iba1 (ab178846), rabbit anti-mouse (ab6728), donkey anti-goat (ab6885), goat anti-rabbit (ab97051) conjugated with horseradish peroxidase (HRP), and goat anti-rabbit, anti-mouse, anti-goat and anti-chicken antibodies conjugated with Alexa Fluor® 405, 488 or Alexa Fluor® 568 were obtained from Abcam (Cambridge, MA). REST expression vectors (REST-myc) and its empty control vector (EV, pCMV6-entry) were from OriGene Technologies (Rockville, MD). Control and expression vectors of a dominant-negative form of REST (DN-REST) were obtained from Addgene (Watertown, MA). The human EAAT2 promoter vector was a gift from Dr. Albert Baldwin (University of North Carolina at Chapel Hill).

2.2. Mice and AAV infusion

The protocols for all animal experiments were approved by the Florida A&M University (FAMU) Institutional Animal Care and Use Committee (IACUC, Tallahassee, FL). Briefly, homozygous $REST^{flox/flox}$ female mice, a gift from Dr. Jenny Hsieh of University of Texas at San Antonio (San Antonio, TX), were used to breed homozygous $REST^{flox/flox}$ mice in FAMU Animal Care Facility. After generating homozygous $REST^{flox/flox}$, mice were housed (3–5 mice/cage) and maintained on a 12-h light/dark cycle at 22 ± 2°C with food, water, and enrichment available *ad libitum*.

After mouse breeding, 24 $REST^{flox/flox}$ homozygous (8-week-old) male mice were randomly assigned into four groups. Mice anesthetized with ketamine/xylazine (100 mg/kg) were placed in a stereotaxic apparatus (6 mice/group). One μl of viral vectors were infused into both sides of the dorsal striatum of the mouse brain using a 10-μl Hamilton syringe (Stoeltling Inc., Wood Dale, IL) mounted to a microinjection pump at a flow rate of 0.2 μl/min. The following stereotaxic injection coordinates were set for dorsal striatum: (from bregma) x = ±1.5 mm (medial-lateral), y = 0.5 mm (anterior-posterior), and z = −2.7 mm (dorsal-ventral). The needle remained in place for five additional minutes before the needle

was slowly withdrawn to prevent reflux of viral vectors. Surgical incisions were closed with a suture, and mice were kept warm with a heating pad before their return to their cages.

After 3 weeks for astrocytic REST deletion, mice were treated according to their designated groups ($n = 6$): (1) AAV5-GFAP-GFP plus vehicle, (2) AAV5-GFAP-GFP plus Mn, (3) AAV5-GFAP-Cre-GFP plus vehicle, and (4) AAV5-GFAP-Cre-GFP plus Mn. Briefly, mice were exposed to Mn ($MnCl_2$ 30 mg/kg, 1 μl per nostril in both nostrils, daily for 21 days) which increases Mn levels about twice, a clinically relevant pathological Mn levels in human brains (Bowman & Aschner, 2014), as described in our previous studies (Pajarillo, Johnson, et al., 2020). Distilled water (ddH_2O) was used as a vehicle. Mice were anesthesized with isoflurane for 3 min during pre- and post-instillation periods to sedate and prevent expulsion of Mn solution or vehicle from the nostrils.

2.3. Open-field, rotarod, and novel object (NO) recognition tests

Twenty-four hours after the last Mn exposure, locomotor activities were assessed in an open field system using Fusion software (version 6.25) for SuperFlex (Omnitech Electronics, Inc., Columbus, OH) as shown in our previous studies (Pajarillo, Johnson, et al., 2020). Each open-field arena measured 27.3 cm × 27.3 cm × 20.3 cm, and was made and covered with Plexiglas material. Each animal were acclimatized in the arena for 3 consecutive days (3 days before the end of the last treatment), then mice groups were tested locomotor activity on the same day. During the test, each mouse was placed in the center of the open field for observation, and the activity measures were recorded for each observed mouse within the 30-min period. The total distance traveled and ambulatory counts were recorded for each subject and used for comparison between groups.

For motor coordination as described in our previous studies (Pajarillo et al., 2020a), mice were trained on the AccuRotor 4-channel rotarod system (Omnitech) for 3 consecutive days prior to the test. Each training session had 3 trials with 5 min resting periods prior to the next trial. On days 0 and 21, each mouse was placed on the rod, and trials were deemed to have started when the rod began to start, with speed gradually increasing from 4 rpm to 40 rpm up to 10 min by 0.1 revolutions/s. The fall latency, time measurement of how fast an experimental subject falls from the rotarod at various speeds was assessed using Fusion software (version 6.3) for AccuRotor (Omnitech). If a mouse persisted on the rod for the entire duration of the trial, the measurement value was recorded for 650 s. The mean duration of fall latency in each group was used for comparison.

For novel object (NO) recognition test, mice were first acclimatized in the open-field arena for 3 consecutive days prior to the actual test. On the actual trial, mice went through a familiarization phase followed by the novel object test. During familiarization, each mouse was exposed to two identical objects (familiar objects, FO) placed on the left and right back corner of the open-field for a 10 min-period, followed by their removal from the arena to set up the NO. During NO test, one FO will be replaced with an item of different texture, shape and color (novel object, NO) on the right back corner of the open-field arena. Mice were placed on the center of the arena with one FO and one NO for a 10-min period. The time spent exploring the NO and FO were recorded with the Fusion software. Mice remained in the chamber until they accumulated at least 30 s of object exploration (Clark,

Zola, & Squire, 2000). NO difference scores and discrimination ratios were calculated and compared between groups (Bevins & Besheer, 2006). A positive NO difference score and a discrimination ratio greater than 0.5 indicates normal function of memory and object retention, whereas negative difference score and discrimination ratios lower than 0.5 depict memory and retention deficit (Bevins & Besheer, 2006).

2.4. Immunohistochemistry (IHC)

IHC procedures were performed as described in the previous studies with slight modifications (Pajarillo, Johnson, et al., 2020). Briefly, brain tissue samples from perfused mice were placed in a 4% paraformaldehyde solution, then in a 30% sucrose solution for 48 h, followed by their immediate snap-freezing. Coronal sections of the mouse brain were obtained for the striatum (1.00 to −1.00 mm) and the substantia nigra (−2.70 to −3.40 mm) from the bregma in 30 μm thickness. Tissue sections (3 mice/group) were prepared for IHC to assess protein expressions of TH, GAD65/67, REST, GFAP, GFP, NeuN, Cre recombinase, and Iba1 in striatum and TH in substantia nigra. In brief, tissue sections were washed twice with PBST (1X PBS, 0.3% Triton X-100), followed by incubation with blocking buffer (1X PBS, 5% normal goat serum, 0.3% Triton X-100) for 1 h at room temperature. Next, tissue sections were incubated with the primary antibody solution in a dark humidity chamber at 4°C overnight. Antibodies for GFAP, NeuN, REST, GFP, Cre, TH, GAD65/67, and Iba1 (1:250 dilution) were diluted in blocking buffer. After overnight incubation, tissue sections were washed with washing buffer, followed by incubation with secondary antibody solution conjugated with Alexa Fluor 405 (blue, DAPI), 488 (green, FITC) and/or 568 (red, TRITC) fluorescent dyes (1:1000 dilution) for 2 h at room temperature in the dark. tissue sections Slides were washed with washing buffer, followed by mounting media and coverslip. Fluorescence intensities of GFAP, NeuN, REST, GFP, Cre, GAD65/67, TH, and Iba1 expressions were assessed in the striatum and TH in substantia nigra from the same histological site of each sample using a Ts2R fluorescence microscope (Nikon Instruments, Melville, NY) and a Leica SPEII confocal microscope (Leica Microsystems Inc., Buffalo Grove, IL), and relative fluorescence intensity was determined as a parameter for TH and GAD expression by Image J software (NIH, Bethesda, MD).

2.5. Cell culture

Primary human astrocytes (#1800, ScienCell Research Laboratories) were cultured as previously described (Pajarillo, Digman, et al., 2021) with a slight modification. Lund human mesencephalic (LUHMES, CRL-2927, ATCC) dopaminergic-like cells were maintained in DMEM/F-12 with 1% N2 supplement (Gibco) and 40 ng/ml basic fibroblast growth factor (PeproTech) and subcultured on culture flasks precoated with 50 μg/ml poly-l-ornithine and 1 μg/ml fibronectin. After plated in 24-well or 6-well tissue culture plates, LUHMES cells were differentiated into morphologically and biochemically mature dopamine-like neurons with a differentiation media containing tetracycline (MilliporeSigma), glial cell–derived neurotrophic factor, and dibutyryl-cAMP (PeproTech), followed by treatment with designated compounds and downstream analysis. Human H4 astrocytes (HTB-148, ATCC) were maintained in DMEM supplemented with 10% fetal bovine serum, 100 U/mL of penicillin, and 100 μg/mL of streptomycin and

maintained at 37°C in a 95% air, 5% CO_2 incubator. Mouse cath.a-differentiated (CAD) catecholaminergic-like cells (MilliporeSigma) were differentiated into morphologically and biochemically mature neurons by replacing them with serum-free media.

2.6. Quantitative PCR (qPCR)

Samples from brain tissues and human astrocytes following the relevant treatment were prepared for qPCR. Total RNA (3 samples/group) were extracted using the RNeasy Mini Kit (Qiagen, Valencia, CA). Two μg of purified RNA was reverse-transcribed to cDNA with a high-capacity cDNA reverse transcription kit (Applied Biosystems, Foster City, CA). Real-time qPCR was performed using the CFX96 (Bio-Rad). The reaction mixture contained 1 μl of each cDNA template, 0.4 μM of primers, and iQ SYBR Green Supermix (Bio-Rad, Hercules, CA). The total reaction volume was 25 μL. The following primers were used for RNA of mouse brain tissues: mouse REST, 5'- ACT TTG TCC TTA CTC AAG CTC-3' (forward) and 5'-CAT TTA AAT GGC TTC TCA CCT G-3' (reverse); mouse GLT-1, 5'-CTC ACT GAC TGT GTT TGG TG-3' (forward) and 5'-GAG GTG CCA CCA GAA CTT TC-3' (reverse); mouse COX-2, 5'-TGC ACT ATG GTT ACA AAA GCT GG-3' (forward) and 5'-TCA GGA AGC TCC TTA TTT CCC TT-3' (reverse); mouse TNF-α, 5'-GAT GAG AAG TTC CCA AAT GGC-3' (forward) and 5'- ACT TGG TGG TTT GCT ACG ACG-3' (reverse); mouse interleukin (IL)-1β, 5'- GAG GAC ATG AGC ACC TTC TTT-3' (forward) and 5'-GCC TGT AGT GCA GTT GTC TAA-3' (reverse); mouse IL-6, 5'-ACA ACC ACG GCC TTC CCT ACT-3' (forward) and 5'-CAC GAT TTC CCA GAG AAC ATG-3' (reverse); mouse GAPDH 5'-CTC ATG ACC ACA GTC CAT GC-3' (forward) and 5'-CAC ATT GGG GGT AGG AAC AC-3' (reverse).

For human astrocytes, human TNF-α, 5'-TGC CCT GTG AGG AGG ACG AA-3' (forward) and 5'-TTC CGA CCC TAA GCC CCC AA-3' (reverse); human COX-2, 5'-TAA GTG CGA TTG TAC CCG GAC-3' (forward) and 5'-TTT GTA GCC ATA GTC AGC ATT GT-3' (reverse); human EAAT2, 5'-CCT GAC GGT GTT TGG TGT CAT- 3' (forward) and 5'-CAA GCG GCC ACT AGC CTT AG- 3' (reverse); human GAPDH, 5'- AAT GGG CAG CCG TTA GGA AA-3' (forward) and 5'-GCG CCC AAT ACG ACC AAA TC-3' (reverse). The qPCR parameters were set for 1 cycle at 95°C for 10 min, 40 cycles at 95°C for 15 s, and 60–65°C for 1 min. GAPDH was used as an internal control. Following qPCR, expression levels of each target gene were detected and quantified using the Bio-Rad CFX Manager version 3.1.

2.7. Western blotting

Samples from astrocyte cultures and tissues from midbrain or striatum (3 samples/group) were homogenized and extracted, followed by bicinchoninic acid (BCA) assay to determine protein concentration. Protein amounts of 15 μg from tissue samples and 30 μg from cell culture per sample were resolved in 8–10% SDS-PAGE gels, followed by immunoblotting for western blot analysis. The following dilution were used for primary antibodies of Cre (1:5,000), REST (1:5,000), TH (1:1,000), COX-2 (1:500), TNF-α (1:500), GFAP (1:1,000), Iba1 (1:1,000), EAAT2/GLT-1 (1:5,000), and HRP-conjugated secondary antibodies (1:5,000). Protein bands were detected with SuperSignal™ West Pico PLUS

Chemiluminescent Substrate (Thermo Scientific, Rockford, IL) and quantified using the Molecular Imager ChemiDoc XRS+ System (Bio-Rad).

2.8. Assays for cell viability and reactive oxygen species (ROS)

For ROS and cell viability assays, differentiated LUHMES cells were treated with the conditioned media (CM) from Mn-exposed primary human astrocytes (PHA), overexpressing either REST or DN-REST. Empty vectors served as control. Briefly, PHA were transfected with EV (pCMV6-entry and TetO-FUW) and plasmid DNA vectors for REST, or DN-REST by electroporation and incubated for 48 h as described in our previous studies (Pajarillo, Digman, et al., 2021). After incubation, REST or DN-REST-overexpressing PHA were exposed to Mn (250 μM, 6 h), followed by replacement of the Mn-containing media with fresh experimental media for an additional of 6 h. Next, the PHA-CM was applied to LUHMES cells to test the effects of astrocytic REST on dopaminergic neuronal cells. LUHMES cells were exposed to the PHA-CM (EV, REST and DN-REST) at designated time period for ROS (3 h) and cell viability (12 h). For ROS assay, LUHMES cells were incubated with 2.5 μM of CM-H2DCFDA (ROS) for 30 min, followed by measurement of green fluorescent dye at an excitation/emission wavelength of 485/527 nm. For cell viability, LUHMES cells were incubated with 1 μg/μL of resazurin for 30 min at 37°C, followed by measurement of red fluorescent dye (resorufin) from live cells at an excitation/emissionwavelength of 530/590 nm. Endpoint intensities of green and red fluorescent dyes were detected using Spectramax® i3x Multi-Mode microplate reader (Molecular Devices, Sunnyvale, CA). The same experimental paradigm was used for human H4 astrocytes and differentiated CAD catecholaminergic cells to determine the effect of astrocytic REST on ROS levels and cell viability in CAD cells.

2.9. Statistical analysis.

The data shown were presented as the mean ± standard deviation (SD). All statistical analyses were performed by two-way analysis of variance (ANOVA), followed by Tukey's *post hoc* tests using the GraphPad Prism Software version 6.0 (San Diego, CA). A *p*-value of less than 0.05 ($p < 0.05$) was considered statistically significant.

3. Results

3.1. Selective deletion of astrocytic REST in the striatum by infusion of AAV viral particles into the dorsal striatum of REST$^{flox/flox}$ mice

Given that Mn preferentially accumulates in globus pallidus and striatum, we modulated astrocytic REST function in dorsal striatal regions by infusing AAV-GFAP-Cre-GFP particles into the dorsal striatal regions of REST-floxed homozygous mouse brains (8 weeks old) to delete REST in striatal astrocytes. First, we confirmed that REST is expressed in striatal astrocytes of REST$^{flox/flox}$ mice by IHC prior to astrocytic REST deletion in the striatum by AAV particles infusion. The imaging data showed that REST is co-localized with GFAP-expressing astrocytes as well as NeuN-expressing neuronal cells (Fig. 1A), indicating that REST is expressed in astrocytes and neurons in the striatum. Next, we deleted REST in astrocytes by infusing AAV5-GFAP-Cre-GFP vectors using AAV5-GFAP-GFP vectors as a control into both sides of the dorsal striatum of the mouse brains to express

Cre recombinase (Cre) (Fig. 1B). The REST-floxed mouse model has an insertion of loxP-flanked sequences on the first coding exon of REST (Gao et al., 2011), and therefore, AAV5-GFAP-Cre vectors will delete a partial exon 1 of the REST gene when Cre is expressed under GFAP promoter control in astrocytes, resulting in selective ablation of REST expression in astrocytes in the infused regions. The control vectors expressing GFP eliminate the potential effects of the AAV vector itself, independent of Cre effects (Albert et al., 2019). Infusion of the AAV5-GFAP-Cre-GFP vectors into the striatum of REST-floxed mice expressed Cre and co-localized with GFAP-expressing astrocytes (Fig. 1C). Expression of Cre recombinase in the striatum was also confirmed by western blotting (Fig. 1D).

As shown in Fig. 1E, astrocytic REST was deleted in striatum by AAV5-GFAP-Cre-GFP vectors, but neurons which are immunostained for NeuN in the same area showed REST expression. Accordingly, astrocytic REST deletion reduced protein levels of REST in the striatum significantly, but not fully, as REST expresses in other cell types such as neurons (Fig. 1F). Notably, Mn treatment itself reduced REST protein levels even in the absence of astrocytic REST deletion (Fig. 1F), indicating that Mn may decrease REST in multiple neural cell types in the striatum.

3.2. Astrocytic REST deletion exacerbates Mn-reduced locomotor activity and motor coordination in mice

Next, we determined if striatal astrocytic REST deletion exacerbates Mn toxicity in the nigrostriatal pathway, focusing on motor function. Striatal astrocytic REST was deleted bilaterally by infusing AAV5-GFAP-Cre vector particles into both sides, which prevent abnormal rotating motor function from a unilateral REST deletion (Iancu, Mohapel, Brundin, & Paul, 2005). First, we determined if astrocytic REST deletion alone could modulate movement of mice 3 weeks after REST deletion via the infusion of AAV5-GFAP-Cre-GFP particles, noting difference in total distance traveled and latency to fall compared to control mice (Fig. 2A,B). Mn exposure via nostril instillation for 3 weeks significantly decreased locomotor activities such as total distance traveled and ambulatory count (number of movement), and astrocytic REST deletion in the striatum further exacerbated the Mn-induced decrease in total number of movements and distance traveled (Fig. 2B–D). Mn impaired motor coordination (Pajarillo, Johnson, et al., 2020; Peres et al., 2015) as it reduced the time for mice to remain on the rotarod (Fig. 2F). Moreover, striatal astrocytic REST deletion alone did not alter motor coordination, but REST deletion exacerbated the Mn-induced reduction in latency to fall from the rotarod (Fig. 2F).

3.3. Striatal astrocytic REST deletion exacerbates Mn-reduced cognitive function in mice

Since Mn has been shown to impair cognitive function (Liang et al., 2016), we determined if striatal astrocytic REST deletion could contribute to Mn-induced cognitive dysfunction in mice. The cognitive function was assessed by the time periods of exploring and interacting with the novel object (Sivakumaran, Mackenzie, Callan, Ainge, & O'Connor, 2018). Striatal astrocytic REST deletion alone did not decrease novel object recognition, but it significantly exacerbated Mn-induced impairment of time on exploring and the time of interaction with a novel object (Fig. 3A), as well as decreased scores in novel object differentiation (Fig. 3B), indicating further impairment of differentiating between novel and familiar objects. Mn

impaired memory function as it reduced discrimination ratio of mice by 60%, which was further decreased in mice with striatal astrocytic REST deletion (Fig. 3C).

3.4. Astrocytic REST deletion exacerbates Mn-induced decrease in TH expression in mice

Mn has been shown to impair locomotor activity and coordination in mice parallel with reduction of TH expression in dopaminergic neurons (Johnson et al., 2018; Pajarillo, Rizor, et al., 2020; Ponzoni, Gaziri, Britto, Barreto, & Blum, 2002). Thus, we tested if striatal astrocytic REST deletion affected Mn-induced reduction in TH expression in the nigrostriatal dopaminergic neurons in the striatum and substantia nigra. Astrocytic REST deletion induced a slight reduction in TH protein and immunofluorescence intensity levels in striatum and substantia nigra (Fig. 4A–D), and Mn exposure significantly decreased TH protein and immunofluorescence intensity levels in both regions. Moreover, striatal astrocytic REST-deletion further exacerbated Mn-induced reduction of TH protein levels in both regions (Fig.4A,C). Mn also reduced TH-positive cells in the substantia nigra in mice infused with the control AAV particles, and striatal astrocytic REST deletion with AAV-Cre particles further decreased the Mn-reduced TH-positive cells in the murine substantia nigra (Fig. 4D). These indicate that astrocytic REST deletion in the striatum where dopaminergic nerve terminals are localized retrogradely damages the nigrostriatal dopaminergic neurons including dopaminergic cell bodies in the substantia nigra.

Since Mn has also been shown to impair gamma-aminobutyric acid (GABA)ergic neuronal cell bodies in the striatum parallel with dopaminergic dysfunction (Stanwood et al., 2009), we determined if astrocytic REST play a role in Mn-induced GABAergic neurotoxicity. The results showed that Mn reduced GAD protein expression in the striatum (Stanwood et al., 2009), and striatal astrocytic REST deletion exacerbated Mn-induced reduction of GAD-expressing cells and immunofluorescence intensity levels in the striatum of mice (Fig. 4E). These findings reveal that astrocytic REST is critical for protecting not only dopaminergic neurons but also GABAergic neurons.

3.5. Striatal astrocytic REST exacerbates Mn-induced inflammation in the striatum and in astrocytes

Next, we investigated a potential molecular mechanisms involved in the role of striatal astrocytic REST in Mn-induced neurotoxicity in the nigrostriatal dopaminergic pathway. First, we examined if astrocytic REST deletion modulates Mn-induced inflammation in striatal astrocytes and microglia. Striatal astrocytic REST deletion increased mRNA and protein levels of the inflammatory mediator COX-2 and cytokine TNF-α in the striatum (Fig. 5A–D). Mn exposure also significantly increased mRNA and protein levels of these inflammatory factors in the striatum and further increased mRNA and protein levels of COX-2 and TNF-α in striatal astrocytic REST deleted mouse brain (Fig. 5A–D). In addition, Mn increased mRNA levels of other proinflammatory cytokines, including IL-1β and IL-6, which were further increased in striatal astrocytic REST deleted mouse brain (Fig. 5E–F). Mn activated astrocytes in the straitum, reflected by increased astrocytic GFAP protein levels and immunofluorescence intensity, an effect that was further exacerbated in striatal astrocytic REST deleted mice (Fig. 5G,H). These observations indicate that astrocytic REST plays an important role in prevention of inflammation. Astrocytic REST deletion also

induced striatal microglial activation, and exacerbated Mn-induced microglial activation in the striatum (Fig. 5I,J).

In order to confirm our findings of the *in vivo* effects of astrocytic REST in inflammation and neuronal toxicity, we first determined if *in vitro* REST modulates Mn-induced expression of proinflammatory genes, including COX-2 and TNF-α in PHA. The results showed that REST inhibition with DN-REST exacerbated Mn-induced mRNA and protein levels of COX-2 and TNF-α in PHA, whereas REST overexpression attenuated these Mn-induced effects in PHA (Fig. 6A–C), indicating that astrocytic REST is critical in protecting against Mn-induced neurotoxicity, at least in part, by modulating gene expression of inflammatory factors in astrocytes.

Next, we used an *in vitro* astrocyte-neuron culture system in which we modulated REST expression in Mn-treated PHA cultures. CM from Mn-exposed PHA, that were overexpressing either REST or DN-REST plasmid vectors in order to increase or reduce REST function, respectively, with empty vector (EV) as a control, were collected and applied to differentiated LUHMES dopaminergic cells. CM from PHA cultures were collected 6 h after Mn-containing media was replaced with a fresh media to eliminate Mn's direct effects on the neuronal culture. CM from Mn-exposed PHA cultures (EV-CM) increased ROS level in LUHMES cells, which was further increased by conditioned media from Mn-treated DN-REST-transfected PHA (DN-REST-CM). However, conditioned media from REST-overexpressed PHA (REST-CM) that were exposed to Mn (250 μM) attenuated the ROS levels in LUHMES cells (Fig. 7A,B). In addition, PHA EV-CM reduced cell viability in LUHMES cells, which was further exacerbated by PHA DN-REST-CM, whereas the PHA REST-CM exposed to Mn attenuated cell viability in LUHMES cells (Fig. 7C). Differentiated CAD cells treated with CM derived from REST and DN-REST-transfected Mn-exposed H4 astrocytes displayed ROS levels and cell viability analogous to those observed in LUHMES cells cultured with CM derived from PHA (Supplementary Figs. 1 and 2).

3.6. Inhibition of astrocytic REST exacerbates Mn-repressed GLT-1 (EAAT2) expression in the striatum and primary astrocyte cultures

Mn toxicity in the striatum is associated with glutamate excitotoxicity (Brouillet et al., 1993) and decreased in GLT-1 mRNA and protein levels in the mouse brain (Johnson et al., 2018; Pajarillo et al., 2018). Since REST modulates astrocytic EAAT2 (GLT-1) (Pajarillo, Digman, et al., 2021), we determined if modulation of REST affects GLT-1 (EAAT2) expression in the mouse brain. The results showed that Mn decreased GLT-1 mRNA and protein levels in the striatum of mice infused with the control vectors of AAV5-GFAP-GFP (Fig. 8A,B), and striatal astrocytic REST deletion by infusion of the AAV5-GFAP-Cre-GFP vectors further exacerbated the Mn-induced decrease in GLT-1 mRNA and protein levels in the striatum. In PHA cultures, REST knockdown with DN-REST also further exacerbated Mn-induced EAAT2 repression, while REST overexpression attenuated Mn-induced reduction in EAAT2 mRNA and protein levels (Fig. 8C,D). REST overexpression and REST inhibiton by DN-REST in H4 astrocytes showed similar results to those in PHA on the EAAT2 expression (Supplementary Fig. 3).

4. Discussion

Our novel findings demonstrate, for the first time, that astrocytic REST deletion in the striatum of the mouse brain exacerbated Mn-induced motor deficit, cognitive impairment and reduction in TH protein levels in the nigrostriatal pathway. At the molecular level, striatal astrocytic REST deletion further elevated the Mn-induced increase in inflammatory factors, such as COX-2, and cytokines including IL-1β, IL-6 and TNF-α, and further decreased the Mn-induced reduction in GLT-1 mRNA and protein levels in the striatum. Mn itself decreased REST protein levels in the murine striatum. These findings suggest that striatal astrocytic REST plays a critical role in Mn-induced neurotoxicity.

Given that Mn neurotoxicity predominantly affects the basal ganglia (Newland et al., 1989), we deleted astrocytic REST specifically in the striatal region to determine astrocytic REST function. We infused AAV5-GFAP-Cre-GFP particles into the dorsal striatum of $REST^{flox/flox}$ mice, corroborating successful astrocytic REST deletion (see Fig. 1) with the GFAP promoter-driven expression of Cre recombinase. The efficacy of the serotype AAV5-GFAP viral vectors in modulating target genes in astrocytes is well established (Griffin et al., 2019; Pajarillo, Johnson, et al., 2020).

It is noteworthy that the Mn exposure paradigm used herein is suitable for studying Mn-induced neurotoxicity, as it induces about two-fold increase in Mn levels in the striatum (Pajarillo, Johnson, et al., 2020). This Mn exposure level is also clinically relevant since human exposure to pathological levels of Mn increases about three-fold compared to the normal Mn levels (Bowman & Aschner, 2014). The pathological signs in this exposure paradigm are also similar to many aspects to human manganism (Lee, 2000) as well as Mn-induced neurotoxic effects in the mouse model (Johnson et al., 2018; Pajarillo et al., 2018).

Mn repressed REST not only in astrocytes but also in other neural cell types, such as neurons (Pajarillo, Rizor, et al., 2020). As shown in Fig. 1E, Mn decreased REST in the striatum of mice with deleted astrocytic REST. In human brains, loss of REST in neurons has been reported to be associated with AD and PD (Kawamura et al., 2019; T. Lu et al., 2014). These findings suggest a critical role of REST, regardless of neural cell type in preventing or slowing down neurodegenerative changes, as well as Mn-induced neurotoxicity.

It is also noteworthy that astrocytic REST is involved in cognitive function in Mn-induced neurotoxicity, as striatal astrocytic REST deletion exacerbated Mn-induced cognitive dysfunction in mice. REST deletion alone did not alter cognitive function, implying that both REST deletion and Mn exposure were required for the phenotype, consistent with gene-environment interaction (Fig. 3B,C). In addition to the effect of Mn on motor function, growing evidence demonstrated that Mn caused cognitive dysfunctions in mice (Wang et al., 2017) and rats (Peres et al., 2015), consistent with our findings on Mn-induced impairment of cognitivefunction characterized by decreased novel object recognition. Furthermore, this effect was worsened following striatal astrocytic REST deletion (Fig. 3). While the mechanistic role of striatum and/or striatal astrocytic REST in cognitive function remains

unclear, it should be noted that the striatum has been implicated in short-term memory tasks, possibly by complex inter-neuronal mechanisms as it receives inputs from different brain regions, including cortex, globus pallidus, substantia nigra, and hippocampus (Rolls, 1994). Further studies are warranted to delineate the mechanistic role of the striatum along with astrocytic REST in Mn-induced cognitive impairment, given that several different neurotransmission inputs associated with striatum might be involved in the Mn-induced cognitive dysregulation (Inoue et al., 1975).

The molecular mechanism of astrocytic REST in Mn-induced neurotoxicity has yet to be well understood, but neuroinflammation and excitoxicity appear to play a role since mRNA and protein levels of inflammatory cytokines and GLT-1 are altered. Striatal astrocytic REST is crucial in protecting from Mn-induced inflammation, as astrocytic REST deletion exacerbated the effects of Mn (Fig. 5). It is well established that Mn preferentially accumulates in astrocytes (Aschner et al., 1992) and increases proinflammatory cytokines such as TNF-α, and ILs, and an inflammatory mediator COX-2 in astrocytes (Filipov, Seegal, & Lawrence, 2005; Liao, Ou, Chen, Chiang, & Chen, 2007; Popichak, Afzali, Kirkley, & Tjalkens, 2018). Proinflammatory cytokines such as TNF-α have been shown to increase COX-2 mRNA and protein levels in astrocytes (Liao et al., 2007), indicating that Mn-induced upregulation of cytokines such as TNF-α may lead to induce COX-2 expression in astrocytes (Fig. 5). Moreover, *in vivo* studies have shown that Mn induced astrogliosis in striatum of mice (Krishna, Dodd, Hekmatyar, & Filipov, 2014) by increasing GFAP expression and nigrostriatal dopaminergic injury, and decreasing TH expression. Indeed, astrocyte-triggered inflammation has been shown to contribute to the pathogenesis of various neurological disorders such as PD, AD, and Mn-induced neurotoxicity (Chinta et al., 2018; Garwood, Pooler, Atherton, Hanger, & Noble, 2011; Popichak et al., 2018). Given these observations, our novel findings on astrocytic REST underscore its protective role against Mn-induced neuroinflammation and ensuing neuronal injury. Although the mechanism of REST-induced decrease in expression of inflammatory mediators is not well understood, we posit that REST may repress the expression of these inflammatory genes at the transcription level, supported by the previous report that REST bound the promoters of *Il1b* (IL-1β), *Ptgs2* (COX-2), and *Tnf*-associated genes in the brain (McGann et al., 2021).

Our findings also revealed that astrocytic REST deletion increased Mn-induced microglial activation as shown by elevated levels of striatal protein Iba-1, a macrophage/microglia-specific calcium-binding protein (Fig. 5H,and I), indicating that astrocytic REST affects microglia, potentially via astrocyte-microglia crosstalk. In agreement, astrocytic REST was a key factor in attenuating microglia activation in an astrocyte-microglia culture model by repressing astrocyte-released cytokines, such as TNF-α and ILs in MPP^+-treated astrocytes (Li et al., 2020).

Although REST could play a role as a repressor of inflammatory genes, REST may also act as an activator on transcriptional regulation. We have recently reported that REST activates EAAT2 (GLT-1) transcription in astrocytes by its direct binding with its *cis*-regulatory element known as RE1 binding sites in the EAAT2 promoter, leading to neuroprotection against Mn-induced dopaminergic neuronal toxicity in an *in vitro* co-culture system (Pajarillo, Digman, et al., 2021). In line with these *in vitro* studies, the present *in vivo* results

show that striatal astrocytic REST deletion decreased mRNA and protein levels of striatal GLT-1, which was further reduced in Mn-treated mice (Fig. 7A,B). The role of REST as an activator in EAAT2 (GLT-1) transcription was confirmed in an *in vitro* astrocyte culture in which REST expression was modulated (Fig. 7C–E), as REST overexpression attenuated Mn-induced reduction of EAAT2 (GLT-1), while REST knockdown further decreased the Mn-induced reduction in EAAT2 (GLT-1) mRNA and protein levels. The mechanism of striatal astrocytic REST deletion-induced EAAT2 (GLT-1) reduction in contributing to Mn-induced neurotoxicity remains to be established, but it could be a consequence of multi-neuronal types of inputs in striatum such as dopaminergic, GABAergic and glutamatergic neurons. It has been previously reported that striatal Mn exposure induced excitotoxic brain lesions in rats, while NMDA receptor antagonist, MK-801 attenuated these Mn effects (Brouillet et al., 1993). Striatal astrocytes play a critical role in maintaining glutamate neurotransmitter homeostasis by reuptaking extracellular glutamate via astrocytic GLT-1 as the striatum receives glutamatergic input from cortex and thalamus (Fonnum, Storm-Mathisen, & Divac, 1981). Reduction of GLT-1 in the striatum along with the elevated extracellular glutamate level have been shown to contribute to nigrostriatal dopaminergic neurodegeration in a MitoPark PD mouse model (Farrand, Gregory, Backman, Helke, & Boger, 2016). Striatal glutamate levels were inversely correlated with locomotor responses to a novel environment, which was associated with dopaminergic dysfunction by altering a dopamine turnover ratio (Shakil et al., 2005). These observations indicate that strital glutamatergic impairment along with astrocytic GLT-1 reduction may contribute to nigrostriatal dopaminergic dysfunction.

Striatal Mn exposure may affect other neuronal types including striatal GABAergic neurons as previous studies have shown that Mn induced the loss of GABAergic neurons in the striatum (Stanwood et al., 2009). Our finding that astrocytic REST deletion exacerbated Mn-reduced protein levels of GAD, which is specific to GABAergic neurons, indicates that astrocytic REST may also be involved in Mn-induced striatal GABAergic neurotoxicity. Given REST's protective role against inflammation and excitotoxicity, astrocytic REST may contribute to the survival and health of many neuronal types involved in behavior, memory, and cognitive functions (C. L. Lu et al., 2014; Ou et al., 2017; Sun et al., 2020).

Taken together, our findings demonstrate that striatal astrocytic REST deletion exacerbated Mn-induced motor deficit and cognitive dysfunction, concomitant with alterations in TH, GLT-1 and proinflammatory mediators and cytokines in the striatum (Fig. 9). Consistent with the previous studies (Kirkley, Popichak, Afzali, Legare, & Tjalkens, 2017; Popichak et al., 2018; Tjalkens, Popichak, & Kirkley, 2017), upon Mn-induced toxicity, astrocytic REST also modulated microglial health and inflammation, given that astrocytic REST deficiency exacerbated Mn-induced microglial activation. These findings suggest that striatal astrocytic REST could be critical in protecting against Mn-induced neurotoxicity by attenuating Mn-induced inflammation and excitotoxicity and offer alternative target for neuroprotection. It appears that REST-induced neuroprotection is mediated not only by astrocytes, but also neurons, as several studies have corroborated that neuronal REST exerted neuroprotection in various experimental models of neurodegenerative diseases, such as AD and PD (T. Lu et al., 2014; McGann et al., 2021; Mozzi et al., 2017; Pajarillo, Rizor, et al., 2020; Ryan et al., 2021; Yu et al., 2013), as well as human subjects (Kawamura et al., 2019; T. Lu et

al., 2014). As for the role of REST in astrocytes, one study has reported that astrocytic REST deletion in the mouse brain exacerbated MPTP (PD-inducing agent in animal models)-induced astrocytic inflammation and dopaminergic neurotoxicity (Li et al., 2020), supporting our findings to underscore the role of astrocytic REST specifically in striatum for protecting against Mn-induced neurotoxicity. Further studies utilizing overexpression of striatal astrocytic REST in Mn-induced neurotoxicity may be necessary to confirm the protective role of astrocytic REST in Mn-induced neurotoxicity. In conclusion, targeting astrocytic REST may afford efficacious therapeutic interventions for the treatment of Mn-induced neurotoxicity as well as other neurodegenerative diseases, at least in part, by modulating proinflammatory factors and glutamate transporter GLT-1 in astrocytes.

Supplementary Material

Refer to Web version on PubMed Central for supplementary material.

Acknowledgment

This work was supported by National Institutes of Health Grants NIEHS R01 ES024756 (to EL), R01 ES031282 (to EL), R01 ES07331 (to MA), NIMHD U54 MD007582 and NCI SC1 CA200519 (to DS). The content is solely the authors' responsibility and does not necessarily represent the official views of the National Institutes of Health.

Reference

Abramovitz L, Shapira T, Ben-Dror I, Dror V, Granot L, Rousso T, … Vardimon L (2008). Dual role of NRSF/REST in activation and repression of the glucocorticoid response. J Biol Chem, 283(1), 110–119. doi:10.1074/jbc.M707366200 [PubMed: 17984088]

Albert K, Voutilainen MH, Domanskyi A, Piepponen TP, Ahola S, Tuominen RK, … Airavaara M (2019). Downregulation of tyrosine hydroxylase phenotype after AAV injection above substantia nigra: Caution in experimental models of Parkinson's disease. J Neurosci Res, 97(3), 346–361. doi:10.1002/jnr.24363 [PubMed: 30548446]

Aschner M, Gannon M, & Kimelberg HK (1992). Manganese uptake and efflux in cultured rat astrocytes. J Neurochem, 58(2), 730–735. doi:10.1111/j.1471-4159.1992.tb09778.x [PubMed: 1729413]

Aschner M, Vrana KE, & Zheng W (1999). Manganese uptake and distribution in the central nervous system (CNS). Neurotoxicology, 20(2–3), 173–180. [PubMed: 10385881]

Banta RG, & Markesbery WR (1977). Elevated manganese levels associated with dementia and extrapyramidal signs. Neurology, 27(3), 213–216. doi:10.1212/wnl.27.3.213 [PubMed: 557755]

Basun H, Forssell LG, Wetterberg L, & Winblad B (1991). Metals and trace elements in plasma and cerebrospinal fluid in normal aging and Alzheimer's disease. J Neural Transm Park Dis Dement Sect, 3(4), 231–258. [PubMed: 1772577]

Bessis A, Champtiaux N, Chatelin L, & Changeux JP (1997). The neuron-restrictive silencer element: a dual enhancer/silencer crucial for patterned expression of a nicotinic receptor gene in the brain. Proc Natl Acad Sci U S A, 94(11), 5906–5911. doi:10.1073/pnas.94.11.5906 [PubMed: 9159173]

Bevins RA, & Besheer J (2006). Object recognition in rats and mice: a one-trial non-matching-to-sample learning task to study 'recognition memory'. Nat Protoc, 1(3), 1306–1311. doi:10.1038/nprot.2006.205 [PubMed: 17406415]

Bouabid S, Fifel K, Benazzouz A, & Lakhdar-Ghazal N (2016). Consequences of manganese intoxication on the circadian rest-activity rhythms in the rat. Neuroscience, 331, 13–23. doi:10.1016/j.neuroscience.2016.06.016 [PubMed: 27316552]

Bowman AB, & Aschner M (2014). Considerations on manganese (Mn) treatments for in vitro studies. Neurotoxicology, 41, 141–142. doi:10.1016/j.neuro.2014.01.010 [PubMed: 24509086]

Brouillet EP, Shinobu L, McGarvey U, Hochberg F, & Beal MF (1993). Manganese injection into the rat striatum produces excitotoxic lesions by impairing energy metabolism. Exp Neurol, 120(1), 89–94. doi:10.1006/exnr.1993.1042 [PubMed: 8477830]

Bruce AW, Lopez-Contreras AJ, Flicek P, Down TA, Dhami P, Dillon SC, … Vetrie D (2009). Functional diversity for REST (NRSF) is defined by in vivo binding affinity hierarchies at the DNA sequence level. Genome Res, 19(6), 994–1005. doi:10.1101/gr.089086.108 [PubMed: 19401398]

Carvalho CF, Oulhote Y, Martorelli M, Carvalho CO, Menezes-Filho JA, Argollo N, & Abreu N (2018). Environmental manganese exposure and associations with memory, executive functions, and hyperactivity in Brazilian children. Neurotoxicology, 69, 253–259. doi:10.1016/j.neuro.2018.02.002 [PubMed: 29432852]

Chen ZF, Paquette AJ, & Anderson DJ (1998). NRSF/REST is required in vivo for repression of multiple neuronal target genes during embryogenesis. Nat Genet, 20(2), 136–142. doi:10.1038/2431 [PubMed: 9771705]

Chinta SJ, Woods G, Demaria M, Rane A, Zou Y, McQuade A, … Andersen JK (2018). Cellular Senescence Is Induced by the Environmental Neurotoxin Paraquat and Contributes to Neuropathology Linked to Parkinson's Disease. Cell Rep, 22(4), 930–940. doi:10.1016/j.celrep.2017.12.092 [PubMed: 29386135]

Chong JA, Tapia-Ramirez J, Kim S, Toledo-Aral JJ, Zheng Y, Boutros MC, … Mandel G (1995). REST: a mammalian silencer protein that restricts sodium channel gene expression to neurons. Cell, 80(6), 949–957. doi:10.1016/0092-8674(95)90298-8 [PubMed: 7697725]

Clark RE, Zola SM, & Squire LR (2000). Impaired recognition memory in rats after damage to the hippocampus. J Neurosci, 20(23), 8853–8860. [PubMed: 11102494]

Emerit J, Edeas M, & Bricaire F (2004). Neurodegenerative diseases and oxidative stress. Biomed Pharmacother, 58(1), 39–46. doi:10.1016/j.biopha.2003.11.004 [PubMed: 14739060]

Farrand AQ, Gregory RA, Backman CM, Helke KL, & Boger HA (2016). Altered glutamate release in the dorsal striatum of the MitoPark mouse model of Parkinson's disease. Brain Res, 1651, 88–94. doi:10.1016/j.brainres.2016.09.025 [PubMed: 27659966]

Filipov NM, Seegal RF, & Lawrence DA (2005). Manganese potentiates in vitro production of proinflammatory cytokines and nitric oxide by microglia through a nuclear factor kappa B-dependent mechanism. Toxicol Sci, 84(1), 139–148. doi:10.1093/toxsci/kfi055 [PubMed: 15601679]

Fonnum F, Storm-Mathisen J, & Divac I (1981). Biochemical evidence for glutamate as neurotransmitter in corticostriatal and corticothalamic fibres in rat brain. Neuroscience, 6(5), 863–873. doi:10.1016/0306-4522(81)90168-8 [PubMed: 6113562]

Gao Z, Ure K, Ding P, Nashaat M, Yuan L, Ma J, … Hsieh J (2011). The master negative regulator REST/NRSF controls adult neurogenesis by restraining the neurogenic program in quiescent stem cells. J Neurosci, 31(26), 9772–9786. doi:10.1523/JNEUROSCI.1604-11.2011 [PubMed: 21715642]

Garwood CJ, Pooler AM, Atherton J, Hanger DP, & Noble W (2011). Astrocytes are important mediators of Abeta-induced neurotoxicity and tau phosphorylation in primary culture. Cell Death Dis, 2, e167. doi:10.1038/cddis.2011.50 [PubMed: 21633390]

Griffin JM, Fackelmeier B, Fong DM, Mouravlev A, Young D, & O'Carroll SJ (2019). Astrocyte-selective AAV gene therapy through the endogenous GFAP promoter results in robust transduction in the rat spinal cord following injury. Gene Ther, 26(5), 198–210. doi:10.1038/s41434-019-0075-6 [PubMed: 30962538]

Guilarte TR, Chen MK, McGlothan JL, Verina T, Wong DF, Zhou Y, … Schneider JS (2006). Nigrostriatal dopamine system dysfunction and subtle motor deficits in manganese-exposed non-human primates. Exp Neurol, 202(2), 381–390. doi:10.1016/j.expneurol.2006.06.015 [PubMed: 16925997]

Huang D, Li Q, Wang Y, Liu Z, Wang Z, Li H, … Huang F (2019). Brain-specific NRSF deficiency aggravates dopaminergic neurodegeneration and impairs neurogenesis in the MPTP mouse model of Parkinson's disease. Aging (Albany NY), 11(10), 3280–3297. doi:10.18632/aging.101979 [PubMed: 31147527]

Iancu R, Mohapel P, Brundin P, & Paul G (2005). Behavioral characterization of a unilateral 6-OHDA-lesion model of Parkinson's disease in mice. Behav Brain Res, 162(1), 1–10. doi:10.1016/j.bbr.2005.02.023 [PubMed: 15922062]

Inoue N, Tsukada Y, & Barbeau A (1975). Behavioral effects in rats following intrastriatal microinjection of manganese. Brain Res, 95(1), 103–124. doi:10.1016/0006-8993(75)90210-3 [PubMed: 1171715]

Johnson J Jr., Pajarillo E, Karki P, Kim J, Son DS, Aschner M, & Lee E (2018). Valproic acid attenuates manganese-induced reduction in expression of GLT-1 and GLAST with concomitant changes in murine dopaminergic neurotoxicity. Neurotoxicology, 67, 112–120. doi:10.1016/j.neuro.2018.05.001 [PubMed: 29778792]

Kawamura M, Sato S, Matsumoto G, Fukuda T, Shiba-Fukushima K, Noda S, … Hattori N (2019). Loss of nuclear REST/NRSF in aged-dopaminergic neurons in Parkinson's disease patients. Neurosci Lett, 699, 59–63. doi:10.1016/j.neulet.2019.01.042 [PubMed: 30684677]

Kirkley KS, Popichak KA, Afzali MF, Legare ME, & Tjalkens RB (2017). Microglia amplify inflammatory activation of astrocytes in manganese neurotoxicity. J Neuroinflammation, 14(1), 99. doi:10.1186/s12974-017-0871-0 [PubMed: 28476157]

Krishna S, Dodd CA, Hekmatyar SK, & Filipov NM (2014). Brain deposition and neurotoxicity of manganese in adult mice exposed via the drinking water. Arch Toxicol, 88(1), 47–64. doi:10.1007/s00204-013-1088-3 [PubMed: 23832297]

Lee JW (2000). Manganese intoxication. Arch Neurol, 57(4), 597–599. doi:10.1001/archneur.57.4.597 [PubMed: 10768639]

Li H, Liu Z, Wu Y, Chen Y, Wang J, Wang Z, … Huang F (2020). The deficiency of NRSF/REST enhances the pro-inflammatory function of astrocytes in a model of Parkinson's disease. Biochim Biophys Acta Mol Basis Dis, 1866(1), 165590. doi:10.1016/j.bbadis.2019.165590 [PubMed: 31706914]

Liang G, Zhang L, Ma S, Lv Y, Qin H, Huang X, … Zou Y (2016). Manganese accumulation in hair and teeth as a biomarker of manganese exposure and neurotoxicity in rats. Environ Sci Pollut Res Int, 23(12), 12265–12271. doi:10.1007/s11356-016-6420-z [PubMed: 26976011]

Liao SL, Ou YC, Chen SY, Chiang AN, & Chen CJ (2007). Induction of cyclooxygenase-2 expression by manganese in cultured astrocytes. Neurochem Int, 50(7–8), 905–915. doi:10.1016/j.neuint.2006.09.016 [PubMed: 17084486]

Lu CL, Tang S, Meng ZJ, He YY, Song LY, Liu YP, … Guo SC (2014). Taurine improves the spatial learning and memory ability impaired by sub-chronic manganese exposure. J Biomed Sci, 21, 51. doi:10.1186/1423-0127-21-51 [PubMed: 24885898]

Lu T, Aron L, Zullo J, Pan Y, Kim H, Chen Y, … Yankner BA (2014). REST and stress resistance in ageing and Alzheimer's disease. Nature, 507(7493), 448–454. doi:10.1038/nature13163 [PubMed: 24670762]

McGann JC, Spinner MA, Garg SK, Mullendorff KA, Woltjer RL, & Mandel G (2021). The Genome-Wide Binding Profile for Human RE1 Silencing Transcription Factor Unveils a Unique Genetic Circuitry in Hippocampus. J Neurosci, 41(31), 6582–6595. doi:10.1523/JNEUROSCI.2059-20.2021 [PubMed: 34210779]

Mozzi A, Guerini FR, Forni D, Costa AS, Nemni R, Baglio F, … Cagliani R (2017). REST, a master regulator of neurogenesis, evolved under strong positive selection in humans and in non human primates. Sci Rep, 7(1), 9530. doi:10.1038/s41598-017-10245-w [PubMed: 28842657]

Newland MC, Ceckler TL, Kordower JH, & Weiss B (1989). Visualizing manganese in the primate basal ganglia with magnetic resonance imaging. Exp Neurol, 106(3), 251–258. doi:10.1016/0014-4886(89)90157-x [PubMed: 2591523]

Ou CY, Luo YN, He SN, Deng XF, Luo HL, Yuan ZX, … Jiang YM (2017). Sodium P-Aminosalicylic Acid Improved Manganese-Induced Learning and Memory Dysfunction via Restoring the Ultrastructural Alterations and gamma-Aminobutyric Acid Metabolism Imbalance in the Basal Ganglia. Biol Trace Elem Res, 176(1), 143–153. doi:10.1007/s12011-016-0802-4 [PubMed: 27491492]

Pajarillo E, Digman A, Nyarko-Danquah I, Son DS, Soliman KFA, Aschner M, & Lee E (2021). Astrocytic transcription factor REST upregulates glutamate transporter EAAT2, protecting

dopaminergic neurons from manganese-induced excitotoxicity. J Biol Chem, 101372. doi:10.1016/j.jbc.2021.101372

Pajarillo E, Johnson J Jr., Kim J, Karki P, Son DS, Aschner M, & Lee E (2018). 17beta-estradiol and tamoxifen protect mice from manganese-induced dopaminergic neurotoxicity. Neurotoxicology, 65, 280–288. doi:10.1016/j.neuro.2017.11.008 [PubMed: 29183790]

Pajarillo E, Johnson J Jr., Rizor A, Nyarko-Danquah I, Adinew G, Bornhorst J, … Lee E (2020). Astrocyte-specific deletion of the transcription factor Yin Yang 1 in murine substantia nigra mitigates manganese-induced dopaminergic neurotoxicity. J Biol Chem, 295(46), 15662–15676. doi:10.1074/jbc.RA120.015552 [PubMed: 32893191]

Pajarillo E, Nyarko-Danquah I, Adinew G, Rizor A, Aschner M, & Lee E (2021). Neurotoxicity mechanisms of manganese in the central nervous system. Adv Neurotoxicol, 5, 215–238. doi:10.1016/bs.ant.2020.11.003 [PubMed: 34263091]

Pajarillo E, Rizor A, Son DS, Aschner M, & Lee E (2020). The transcription factor REST up-regulates tyrosine hydroxylase and antiapoptotic genes and protects dopaminergic neurons against manganese toxicity. J Biol Chem, 295(10), 3040–3054. doi:10.1074/jbc.RA119.011446 [PubMed: 32001620]

Palm K, Belluardo N, Metsis M, & Timmusk T (1998). Neuronal expression of zinc finger transcription factor REST/NRSF/XBR gene. J Neurosci, 18(4), 1280–1296. [PubMed: 9454838]

Palm K, Metsis M, & Timmusk T (1999). Neuron-specific splicing of zinc finger transcription factor REST/NRSF/XBR is frequent in neuroblastomas and conserved in human, mouse and rat. Brain Res Mol Brain Res, 72(1), 30–39. doi:10.1016/s0169-328x(99)00196-5 [PubMed: 10521596]

Peres TV, Eyng H, Lopes SC, Colle D, Goncalves FM, Venske DK, … Leal RB (2015). Developmental exposure to manganese induces lasting motor and cognitive impairment in rats. Neurotoxicology, 50, 28–37. doi:10.1016/j.neuro.2015.07.005 [PubMed: 26215118]

Ponzoni S, Gaziri LC, Britto LR, Barreto WJ, & Blum D (2002). Clearance of manganese from the rat substantia nigra following intra-nigral microinjections. Neurosci Lett, 328(2), 170–174. doi:10.1016/s0304-3940(02)00464-0 [PubMed: 12133581]

Popichak KA, Afzali MF, Kirkley KS, & Tjalkens RB (2018). Glial-neuronal signaling mechanisms underlying the neuroinflammatory effects of manganese. J Neuroinflammation, 15(1), 324. doi:10.1186/s12974-018-1349-4 [PubMed: 30463564]

Poulin JF, Tasic B, Hjerling-Leffler J, Trimarchi JM, & Awatramani R (2016). Disentangling neural cell diversity using single-cell transcriptomics. Nat Neurosci, 19(9), 1131–1141. doi:10.1038/nn.4366 [PubMed: 27571192]

Przedborski S, & Vila M (2001). The last decade in Parkinson's disease research. Basic sciences. Adv Neurol, 86, 177–186. [PubMed: 11553976]

Rolls ET (1994). Neurophysiology and cognitive functions of the striatum. Rev Neurol (Paris), 150(8–9), 648–660. [PubMed: 7754303]

Rothstein JD, Dykes-Hoberg M, Pardo CA, Bristol LA, Jin L, Kuncl RW, … Welty DF (1996). Knockout of glutamate transporters reveals a major role for astroglial transport in excitotoxicity and clearance of glutamate. Neuron, 16(3), 675–686. doi:10.1016/s0896-6273(00)80086-0 [PubMed: 8785064]

Ryan BJ, Bengoa-Vergniory N, Williamson M, Kirkiz E, Roberts R, Corda G, … Wade-Martins R (2021). REST Protects Dopaminergic Neurons from Mitochondrial and alpha-Synuclein Oligomer Pathology in an Alpha Synuclein Overexpressing BAC-Transgenic Mouse Model. J Neurosci, 41(16), 3731–3746. doi:10.1523/JNEUROSCI.1478-20.2021 [PubMed: 33563726]

Schoenherr CJ, & Anderson DJ (1995). The neuron-restrictive silencer factor (NRSF): a coordinate repressor of multiple neuron-specific genes. Science, 267(5202), 1360–1363. doi:10.1126/science.7871435 [PubMed: 7871435]

Schoenherr CJ, Paquette AJ, & Anderson DJ (1996). Identification of potential target genes for the neuron-restrictive silencer factor. Proc Natl Acad Sci U S A, 93(18), 9881–9886. doi:10.1073/pnas.93.18.9881 [PubMed: 8790425]

Shakil SS, Holmer HK, Moore C, Abernathy AT, Jakowec MW, Petzinger GM, & Meshul CK (2005). High and low responders to novelty show differential effects in striatal glutamate. Synapse, 58(3), 200–207. doi:10.1002/syn.20198 [PubMed: 16138315]

Sivakumaran MH, Mackenzie AK, Callan IR, Ainge JA, & O'Connor AR (2018). The Discrimination Ratio derived from Novel Object Recognition tasks as a Measure of Recognition Memory Sensitivity, not Bias. Sci Rep, 8(1), 11579. doi:10.1038/s41598-018-30030-7 [PubMed: 30069031]

Stanwood GD, Leitch DB, Savchenko V, Wu J, Fitsanakis VA, Anderson DJ, … McLaughlin B (2009). Manganese exposure is cytotoxic and alters dopaminergic and GABAergic neurons within the basal ganglia. J Neurochem, 110(1), 378–389. doi:10.1111/j.1471-4159.2009.06145.x [PubMed: 19457100]

Sun Y, He Y, Yang L, Liang D, Shi W, Zhu X, … Ou, C. (2020). Manganese induced nervous injury by alpha-synuclein accumulation via ATP-sensitive K(+) channels and GABA receptors. Toxicol Lett, 332, 164–170. doi:10.1016/j.toxlet.2020.07.008 [PubMed: 32659473]

Tjalkens RB, Popichak KA, & Kirkley KA (2017). Inflammatory Activation of Microglia and Astrocytes in Manganese Neurotoxicity. Adv Neurobiol, 18, 159–181. doi:10.1007/978-3-319-60189-2_8 [PubMed: 28889267]

Tong Y, Yang H, Tian X, Wang H, Zhou T, Zhang S, … Chui D (2014). High manganese, a risk for Alzheimer's disease: high manganese induces amyloid-beta related cognitive impairment. J Alzheimers Dis, 42(3), 865–878. doi:10.3233/JAD-140534 [PubMed: 24961945]

Wang D, Zhang J, Jiang W, Cao Z, Zhao F, Cai T, … Luo W (2017). The role of NLRP3-CASP1 in inflammasome-mediated neuroinflammation and autophagy dysfunction in manganese-induced, hippocampal-dependent impairment of learning and memory ability. Autophagy, 13(5), 914–927. doi:10.1080/15548627.2017.1293766 [PubMed: 28318352]

Yu M, Suo H, Liu M, Cai L, Liu J, Huang Y, … Huang F (2013). NRSF/REST neuronal deficient mice are more vulnerable to the neurotoxin MPTP. Neurobiol Aging, 34(3), 916–927. doi:10.1016/j.neurobiolaging.2012.06.002 [PubMed: 22766071]

Zhao F, Cai T, Liu M, Zheng G, Luo W, & Chen J (2009). Manganese induces dopaminergic neurodegeneration via microglial activation in a rat model of manganism. Toxicol Sci, 107(1), 156–164. doi:10.1093/toxsci/kfn213 [PubMed: 18836210]

Zoni S, Bonetti G, & Lucchini R (2012). Olfactory functions at the intersection between environmental exposure to manganese and Parkinsonism. J Trace Elem Med Biol, 26(2–3), 179–182. doi:10.1016/j.jtemb.2012.04.023 [PubMed: 22664337]

Main points

- Striatal astrocytic REST deletion exacerbates Mn-induced toxicity in basal ganglia
- Striatal astrocytic REST deletion exacerbates Mn-induced neuroinflammation
- Astrocytic REST is protective against Mn-induced GLT-1 dysregulation

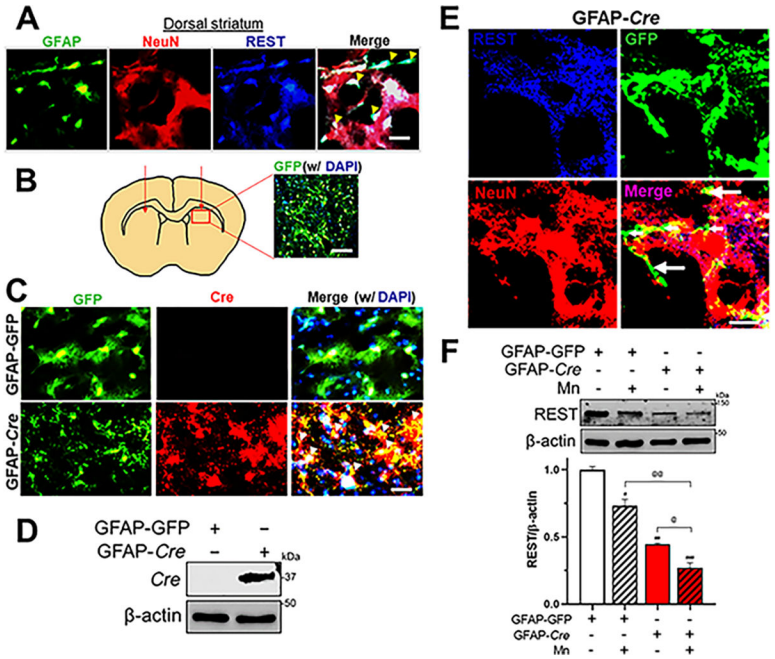

Figure 1. Validation of astrocytic REST deletion by infusion of AAV viral particles into the dorsal striatum of mouse brain.

A, three weeks after infusion of AAV viral particles into the dorsal striatum of the REST$^{flox/flox}$ mouse brain to delete astrocytic REST, striatal sections were examined for immunohistochemical validation as described in the Methods section using antibodies for GFAP, NeuN and REST (green, GFAP; red, NeuN; blue, REST; ×60 magnification, scale = 25 μm). Yellow arrows, REST expression co-localized with GFAP-expressing astrocytes in striatum. B, cells expressing GFP (green, ×4 magnification, scale = 250 μm) show the site of AAV vector infusion in striatal dopaminergic terminal regions. C, co-localization of GFP (green, AAV-infused astrocytes) and Cre (red, Cre-recombinase) in the striatum, indicating astrocytic Cre expression (×40 magnification,, scale = 50 μm). White arrows show Cre co-expressing with GFP in astrocytes. D, protein expression of Cre in the mouse striatum by immunoblotting. E, imagings of GFP (green) for astrocytes, NeuN (red) for neurons, and REST (blue) (×60 magnification, scale = 25 μm). White arrows show REST deletion in astrocytes. F, after Mn exposure, striatal tissues were assessed for REST protein by western blotting. β-actin was used as a loading control of protein. $^{\#\#}$, $p < 0.01$; $^{\#\#\#}$, $p < 0.001$ compared with the controls; $^{@}$, $p < 0.05$; $^{@@}$, $p < 0.01$ compared with each other (two-way ANOVA followed by Tukey's post hoc test; $n = 3$). Data are expressed as mean ± S.D.

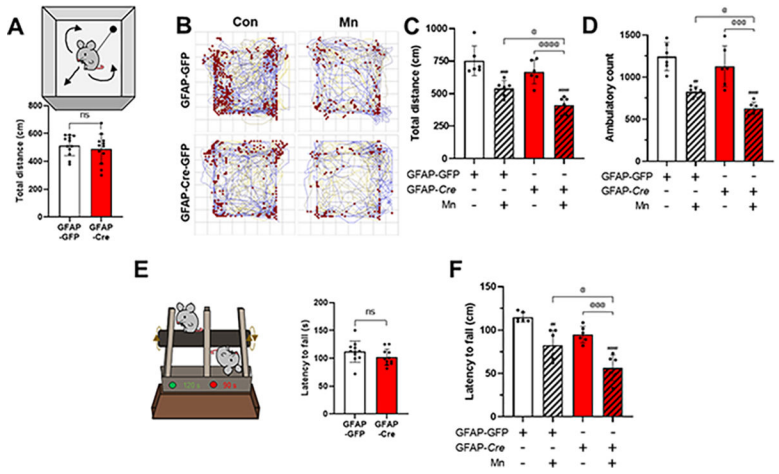

Figure 2. Deletion of astrocytic REST in the mouse striatum exacerbates Mn-induced impairment of locomotor activity and motor coordination.

A, three weeks after AAV5 particle infusion, locomotor activity was measured in the open field using SuperFlex system as described in the Methods section. B-D, After Mn exposure ($MnCl_2$, 30 mg/kg, intranasal instillation, daily for 3 weeks), locomotor activity was assessed by open-field traces (B), total distance traveled (C) and ambulatory count (D). Traces depict movement and red dots indicate the location of vertical activity in the open-field arena. E-F, motor coordination assessed by fall latency as time spent on the rotating rod in mice. $^{\#}$, $p < 0.05$; $^{\#\#\#}$, $p < 0.001$; $^{\#\#\#\#}$, $p < 0.0001$ compared with the controls; $^{@}$, $p < 0.05$; $^{@@}$, $p < 0.01$; $^{@@@@}$, $p < 0.0001$ compared with each other (two-way ANOVA followed by Tukey's post hoc test; $n = 6$). Data are expressed as mean ± S.D.

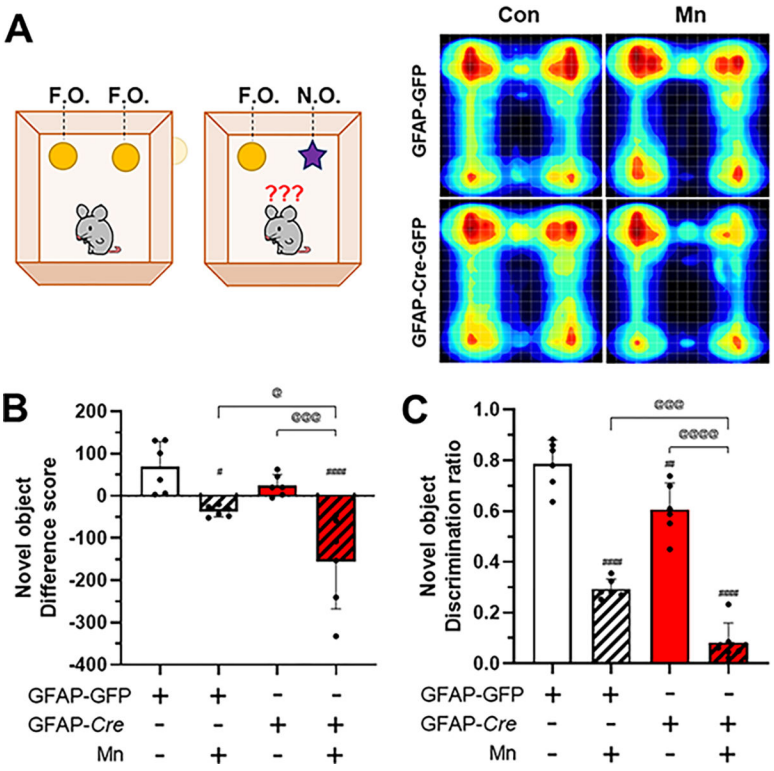

Figure 3. Mn decreases cognitive function and deletion of striatal astrocytic REST exacerbates Mn-induced impairment of cognitive function.

A, after Mn exposure ($MnCl_2$, 30 mg/kg, nostril instillation, daily for 3 weeks), novel object recognition was assessed as described in the Methods section. A, NO recognition was assessed in mice by measuring time spent on the novel object (NO, top-right) compared to the familiar (FO, top-left). Heatmap showing from blue to yellow-red depicts patterns of mouse movement depending on time spent around a specific object or area in the arena. Red shows highest time spent in one area. B-C, NO difference score (B) and discrimination ratio (C) were analyzed from the time spent in both objects in the open-field arena. $^{\#}$, $p < 0.05$; $^{\#\#\#\#}$, $p < 0.0001$ compared with the controls; $^{@}$, $p < 0.05$; $^{@@@}$, $p < 0.001$, $^{@@@@}$, $p < 0.0001$ compared with each other (two-way ANOVA followed by Tukey's post hoc test; $n = 6$). Data are expressed as mean ± S.D.

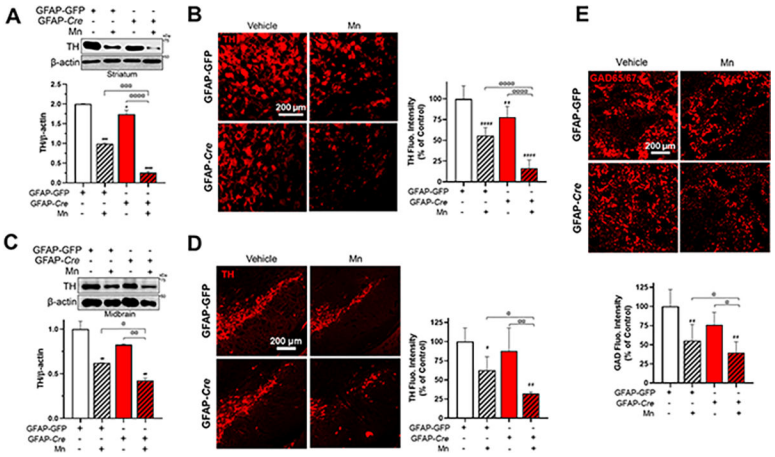

Figure 4. Deletion of striatal astrocytic REST exacerbates Mn-induced decrease of TH expression in striatum and substantia nigra/midbrain as well as GAD expression in the striatum of mice.

A-B, after Mn exposure ($MnCl_2$, 30 mg/kg, nostril instillation, daily for 3 weeks), striatum (A,B) and midbrain (C,D) regions of mouse brains were analysed for TH protein levels by western blotting and IHC. β-actin was used as a loading control. E, after Mn treatment, coronal sections from striatum were immunostained for GAD65/67 as described in the Methods section. Protein expressions of TH in striatum and substantia nigra as well as GAD in striatum were visualized with red fluorescence signals (TRITC) (×10 magnification). Fluorescence intensity of TH and GAD are shown as a percentage of the control. *, $p < 0.05$; **, $p < 0.01$; ***, $p < 0.001$; ****, $p < 0.0001$; #, $p < 0.05$; ##, $p < 0.01$; ####, $p < 0.0001$, compared with the controls; @, $p < 0.05$; @@, $p < 0.01$; @@@, $p < 0.001$; @@@@, $p < 0.0001$ compared with each other (two-way ANOVA followed by Tukey's post hoc test; $n = 3$). Data are expressed as mean ± S.D.

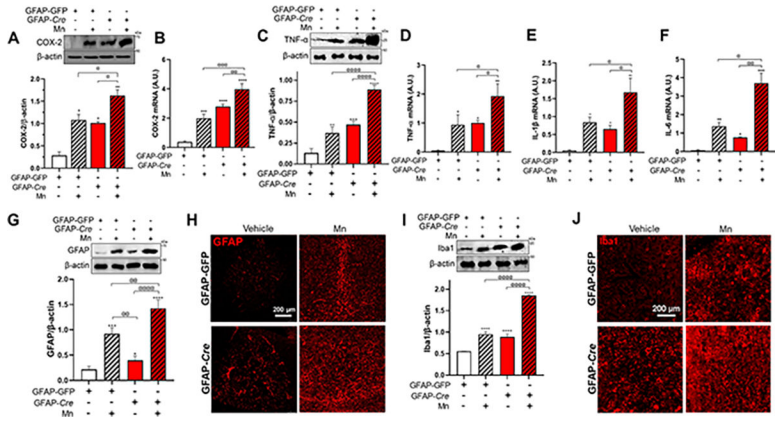

Figure 5. Deletion of striatal astrocytic REST exacerbates Mn-induced expression of proinflammatory factors in the mouse striatum.

After Mn exposure ($MnCl_2$, 30 mg/kg, nostril instillation, daily for 3 weeks), striatal tissues were analyzed for mRNA and protein levels by qPCR and WB, respectively. A-F, Mn increased protein and mRNA levels of COX-2 (A,B) and TNF-α (C,D) as well as mRNA levels of IL-1β, and IL-6 (E,F), which were exacerbated by striatal astrocytic REST deletion in the mouse striatum. G-H, Mn increased GFAP protein levels (G) and GFAP-positive cells (H). I-J, Mn increased microglia Iba1 protein levels (I) and Iba1-positive cells (J) in the striatum, which were exacerbated by striatal astrocytic REST deletion. GAPDH and β-actin were used as loading controls for mRNA and protein, respectively. *, $p < 0.05$; **, $p < 0.01$; ***, $p < 0.001$; ****, $p < 0.0001$, compared with the controls; $^{@}$, $p < 0.05$; $^{@@}$, $p < 0.01$; $^{@@@}$, $p < 0.001$; $^{@@@@}$, $p < 0.0001$ compared with each other (two-way ANOVA followed by Tukey's post hoc test; $n = 3$). Data are expressed as mean ± S.D.

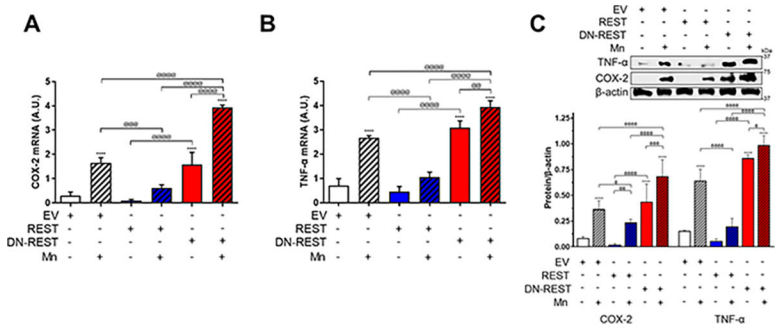

Figure 6. The *in vitro* modulation of astrocytic REST expression alters Mn-induced production of proinflammatory factors in primary human astrocytes (PHA).

PHA were transfected with empty vector (EV), REST or dominant-negative (DN)-REST vectors to modulate REST expression, followed by exposure to Mn (250 μM, 12 h). PHA were analyzed for expression of mRNA levels of COX-2 (A) and TNF-α (B), and protein levels of COX-2 and TNF-α (C). GAPDH and β-actin were used as loading controls for mRNA and protein, respectively. ****, $p < 0.0001$, compared with the controls; @, $p < 0.05$; @@, $p < 0.01$; @@@, $p < 0.001$; @@@@, $p < 0.0001$ compared with each other (two-way ANOVA followed by Tukey's post hoc test; $n = 3$). Data are expressed as mean ± S.D. The data shown are representative of three independent experiments.

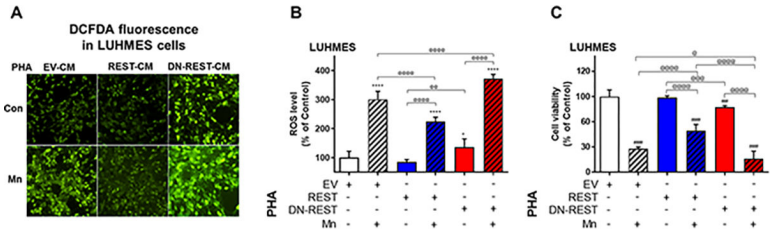

Figure 7. The modulation of astrocytic REST expression alters Mn-induced neurotoxicity in astrocyte-neuron co-culture.

PHA were transfected with empty vector (EV), REST or dominant negative (DN)-REST vectors to modulate REST expression, followed by exposure to Mn (250 μM). After Mn exposure of PHA cultures for 6 h, the media was replaced with fresh media and incubated for 6 h prior to media collection as described in the Methods. This conditioned media (CM) were applied to differentiated LUHMES cells. After CM exposure (3 h for ROS; 12 h for cell viability), LUHMES cells were analyzed for ROS levels by CM-H2DCFDA fluorescence (A, imaging; B, quantification) and cell viability was determined by resazurin assays (C). *, $p < 0.05$; ****, $p < 0.0001$; ###, $p < 0.001$; ####, $p < 0.0001$, compared with the controls; @, $p < 0.05$; @@, $p < 0.01$; @@@, $p < 0.001$; @@@@, $p < 0.0001$ compared with each other (two-way ANOVA followed by Tukey's post hoc test; $n = 6$). Data are expressed as mean ± S.D. The data shown are representative of three independent experiments.

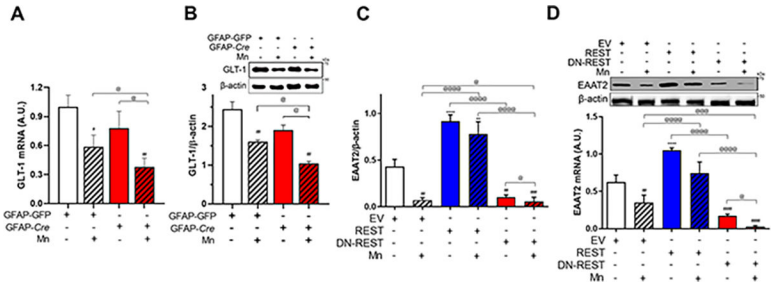

Figure 8. Astrocytic REST deletion exacerbates Mn-induced decrease in astrocytic glutamate transporter GLT-1 (EAAT2 in human) in the mouse striatum as well as PHA.

A-B, after striatal astrocytic REST deletion with following Mn exposure, striatal tissues were analyzed for mRNA and protein levels by qPCR and WB, respectively. A-B, Mn decreased mRNA (A) and protein (B) levels of GLT-1, whereas astrocytic REST deletion exacerbated these Mn effects on GLT-1 in the striatum. C-D, PHA were transfected with EV, REST or DN-REST vectors to modulate REST expression, followed by exposure to Mn (250 μM, 12h). Inhibition of REST further decreased Mn-induced reduction of EAAT2 mRNA (C), and protein (D) levels, whereas REST overexpression attenuated the Mn's effects in PHA. GAPDH and β-actin were used as loading controls for mRNA and protein, respectively. **, $p < 0.01$; ****, $p < 0.0001$; $^{\#}$, $p < 0.05$; $^{\#\#}$, $p < 0.01$; $^{\#\#\#\#}$, $p < 0.0001$, compared with the controls; $^{@}$, $p < 0.05$; $^{@@@}$, $p < 0.001$; $^{@@@@}$, $p < 0.0001$ compared with each other (two-way ANOVA followed by Tukey's post hoc test; $n = 3$). Data are expressed as mean ± S.D.

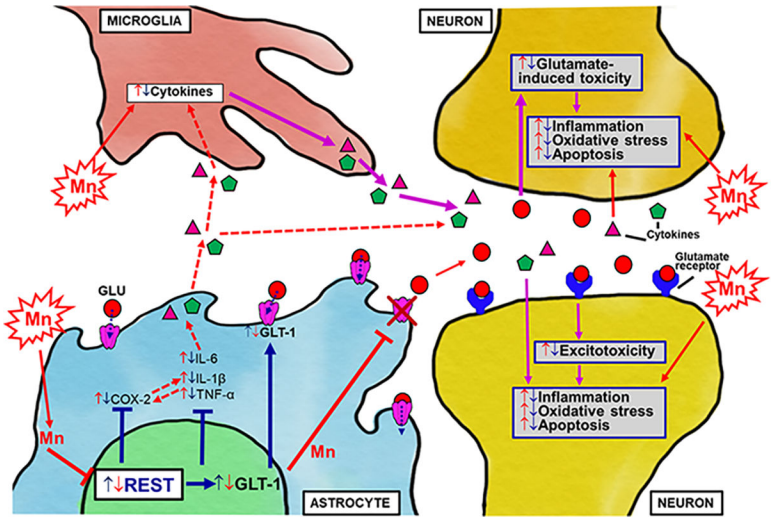

Figure 9. Schematic diagram of the proposed mechanism of striatal astrocytic REST-induced protection against Mn's neurotoxicity in mice.

Striatal astrocytic REST (blue lines) may exert protective effects against neurotoxicity by attenuating the Mn-induced production of inflammatory mediators and decrease in GLT-1 expression in astrocytes. Mn (red lines) induces oxidative stress, inflammation, excitotoxicity and apoptosis in the striatum, at least in part by Mn's reduction of astrocytic REST, propagating its toxicity in different neural cell types including neurons, microglia, and astrocytes directly and indirectly via cross-talks between cells, leading to inflammatory neurotoxicity (magenta arrow). GLU, glutamate; GLT-1 glutamate transporter 1; REST, repressor element 1 silencing transcription factor; COX-2, cyclooxygenase 2; TNF-α, tumor necrosis factor alpha; IL-1β, interleukin-1β; IL-6, interleukin-6.